Study of the Ion Transfer of Quaternary Ammonium Ions by SWV

Joaquín Rodríguez-López[1] and Marcelo Videa[2],*

[1] Department of Chemistry, University of Illinois at Urbana-Champaign, 505 South Mathews Ave. Urbana, IL 61801.
joaquinr@illinois.edu
[2] Departmento de Química, Tecnológico de Monterrey, Campus Monterrey, Av. Garza Sada 2501 Sur, Monterrey, N.L., 64849,
México. mvidea@itesm.mx

Abstract. Simple transfer across the water/nitrobenzene interface of three model quaternary ammonium cations: Tetramethylammonium (TMA^+), Choline (Ch^+) and Tetrabutylammonium (TBA^+), was followed by Square Wave Voltammetry (SWV) which constitutes a more sensitive approach to ionic quantification compared to other conventional techniques. A linear and reproducible response was observed in the range of 10 to 100 μM. Detection limits obtained by the ULA-2 method were 5.9, 10.7 and 13.8 μM for the mentioned ions, respectively. The simultaneous and independent analysis of two ions with different hydrophilic characters such as TBA^+ and Ch^+ is achieved by direct inspection of the resulting voltammograms after background subtraction. We report the particular effect of temperature in the SWV response studied in the range from 288 K to 313 K. The differential peak current shows a significant linear increase with increasing temperatures while background currents show no variation, thus turning the combined enhancement of using a differential pulse method at an optimal temperature into a significant option for quaternary ammonium ion quantitative analysis.
Key words: Square Wave Voltammetry, Quaternary Ammonium Ions, Ion transfer, Choline.

Resumen. La transferencia simple a través de la interfaz agua/nitrobenceno de tres cationes modelo de amonio cuaternario: tetrametilamonio (TMA^+), colina (CH^+) y tetrabutilamonio (TBA^+), fue seguida por voltamperometría de onda cuadrada (VOC), una técnica que proporciona mayor sensibilidad en la cuantificación en comparación con otras técnicas convencionales. Se observó una respuesta lineal y reproducible en el intervalo de 10 a 100 µM. Los límites de detección obtenidos por el método ULA-2 fueron 5.9, 10.7 y 13.8 mM para los iones mencionados, respectivamente. El análisis simultáneo e independiente de dos iones con diferentes caracteres hidrófilos tales como TBA^+ y Ch^+ se logra mediante la inspección directa de los voltamogramas resultantes después de la sustracción de fondo. Se presenta el efecto particular de la temperatura sobre la respuesta de SWV estudiado en el intervalo de 288 K a 313 K. El pico de corriente diferencial muestra un aumento lineal significativo con el aumento de la temperatura mientras que las corrientes de fondo no muestran ninguna variación, convirtiendo así la combinación de la aplicación de un método de pulso diferencial y una temperatura óptima en una opción notable para el análisis cuantitativo del ion amonio cuaternario.
Palabras clave: Voltamperometría de onda cuadrada, iones cuaternarios de amonio, transferencia de iones, colina.

Introduction

The study of the ion transfer across the interface between two immiscible electrolyte solutions (ITIES) opens the possibility to novel applications in the field of electrochemical analysis where its importance has been recognized extensively [1-6]. The non-destructive properties of the transfer process on an ionic sample and its natural selectivity towards charged species are of much interest in the sense that the problems associated with more conventional analytical techniques can be overcome, e.g. the presence of neutral matrix interferences. This is of major importance to applications such as biological or environmental analysis. Indeed, quaternary ammonium compounds are substances widely used in the industry and household due to their antiseptic, tensoactive and herbicidal properties [7], and are also present in biological systems as neurotransmitter-related agents [8, 9].

Chromatographic methods have been described for the analysis of quaternary ammonium compounds: thin layer chromatography [10], ion/ion-pair chromatography [11, 12, 13] and gas chromatography with a surface ionization detector [14]. While the latter has proven good limits of detection, the identification of the compounds is indirect and the maintenance of the equipment is costly. Electrochemistry based chromato-

graphic methods such as Capillary Electrophoresis have been successfully used to identify and quantify quaternary ammonium compounds in disinfectants and antibacterials [15, 16, 17], pharmaceutical preparations [18-21] and herbicides in preparations and water [22, 23]. However, the attainment of micromolar or nanomolar detection limits is usually restricted to those methods that couple mass spectrometry, thus increasing the cost of operation and making the instrumentation required to perform the analysis unachievable to many laboratories. Electrochemical methods such as those allowed by amperometry of the ion transfer across an ITIES offer on the other hand a cheap and simple alternative to the analysis of quaternary ammonium compounds; they are also beyond the conventional potentiometric analysis [9, 24]. The analytical value of these techniques has been recognized almost since its beginnings [6, 26] and the field continues to be explored and enriched with new applications [4, 5]. Most of what is done however is based on conventional techniques such as cyclic voltammetry; in order to compete with other methods of analysis like the ones described in the previous paragraph, enhancements in the analytical performance of the electrochemical methods must be achieved. Such enhancements may well come from the use of pulse voltammetric methods such as square wave voltammetry.

Square Wave Voltammetry (SWV) is a suitable technique to study the ion transfer across an ITIES since it allows an enhancement in the sensitivity of the signal from the analyte and a partial suppression of the background signal at moderate scan rates, providing easiness of interpretation of peak parameters. Although the use of this technique has been reported before [27, 28, 29, 30] the present work makes a contribution in recognizing important parameters for implementing this technique as a complement to cyclic voltammetry and reports a significant temperature effect enhancement of the peak current against the background current. In order to understand better the electrochemical behavior of the system, the scope of this study is limited to the simple ion transfer of quaternary ammonium ions. Three model ions, choline (Ch^+), tetramethylammonium (TMA^+) and tetrabutylammonium (TBA^+) were chosen on the grounds of their electrochemical behavior at the water/nitrobenzene ITIES. Our intention is to focus the study to a general case, whereas particular applications for these or other quaternary ammonium ions can draw benefits from the results presented.

Results and Discussion

In the cell configuration described in the experimental section, a scan towards more positive potential values than that of the initial potential will allow the transference of a positively charged ion from the initial water phase into the nitrobenzene phase; hydrophilic ions will transfer at higher potential values while hydrophobic ions will transfer at lower potential values. Figure 1 shows the transfer of TMA^+ at different concentrations; the wave for such transference can be recognized at high potentials with respect to the initial 0.1 V. As expected, there is a background current that arises from the transference of the ions of both supporting electrolytes. This background current is seen to increase sharply at lower potentials than 0.15 V and higher potentials than 0.75 V, rendering a potential window of approximately 0.6 V. Upon polarization beyond
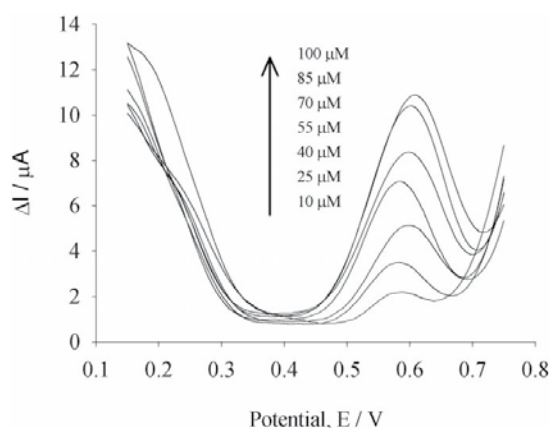
these limits, there is a saturation of the signal that leads to distorted voltammograms which are in general non-reproducible. Figure 1 shows the expected behavior of increasing differential peak current at increasing analyte concentrations in the aqueous phase according to equation 1 for SWV [31]:

$$\Delta I_p = 0.9653 \; nFc^*AD_i^{1/2}f^{1/2} \tanh(\zeta_{SW}/2) \qquad (1)$$

where ΔI_p represents the peak differential current, n is the number of charges transferred, F is Faraday's constant, c^* is the bulk concentration of the analyte in this case in the aqueous phase, D_i is the diffusion coefficient of the species, f the square wave frequency and the term ζ_{SW} is equal to $nFE_{SW} = RT$ where E_{SW} is the square wave pulse amplitude, R is the ideal gas constant and T is the temperature. Figure 2 shows the transfer of both TBA^+ and Ch^+ within the same set of runs; the signal at lower potentials corresponds to TBA^+ while the one at higher potentials corresponds to the transfer of the less polar Ch^+ in accordance to their electrochemical potentials. It is important to mention that the transfer of these ions across the interface within the same run without interference from each other is an important feature that SWV allows. In the direction chosen for the potential scan, the wave from the transference of TBA^+ fades out to the background level and then an independent signal from Ch^+ can be observed. In the case of this set of voltammograms, the background current had to be subtracted from the raw signal in order to obtain a recognizable wave for TBA^+ due to the overlap of its signal with the limits of the potential window. When such an overlapping is small, as in the case for both ions, the subtraction of the background current allows the acquisition of the voltammograms whose characteristics are fully described by equation 1. This however is limited to a certain range of potentials since the transfer of the supporting electrolytes (in much higher concentration) renders the signal undistinguishable. Table 1 summarizes the mean transference potentials obtained from the SW voltammograms.
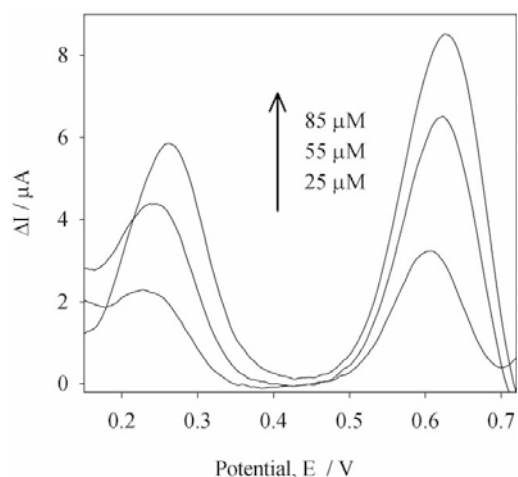

Figure 1. Concentration dependence of the SWV signal for the transfer of TMA^+ at several concentrations. The waves for $[TMA^+] = 10\mu M$ and $25\mu M$ are displaced +10mV for clarity.

Figure 2. Concentration dependence of the SWV signal for the transfer of TBA^+ and Ch^+ at increasing concentrations (corresponding to both transferring ions) within the same run.

Table 1. Measured mean potentials for the transfer of the selected quaternary ammonium ions.

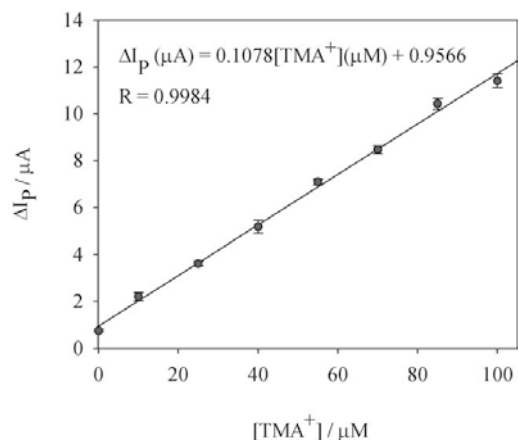| Species	Mean potential/V	Mean deviation/V
TMA+	0.576	0.012
Ch+	0.614	0.009
TBA+	0.236	0.015

Table 2. Typical peak widths at half-height ($W_{1/2}$) for the transference of TMA$^+$ at different concentrations.

[TMA+]/μM	$W_{1/2}$/mV
10	88
25	112
40	116
55	120
70	121
85	136
100	128

Figure 3. Peak differential current versus concentration plot for the transference of TMA$^+$. The value of the background is added to the set of data in accordance to the ULA2 method. Each point corresponds to a total of 6 runs in 2 different experiments; error bars indicate $\pm$ standard deviation.

Figure 4. Peak differential current versus concentration plot for the transference of Ch$^+$. The value of the background is added to the set of data in accordance to the ULA2 method. Each point corresponds to a total of 6 runs in 2 different experiments; error bars indicate $\pm$ standard deviation.

As expected, Ch$^+$ which is the most polar of the three ions presents the highest transference potential while TBA$^+$ transfers at a potential 400mV lower, covering therefore the practical range of the electrochemical window. As Figure 1 and Figure 2 evidence, there is a displacement on the peak potential for all runs which is further noted by the mean deviation in Table 1. In the ideal case, such a displacement is not expected as the peak signal should be independent of the concentration of analyte; however, the fact that only 80% compensation in the potential drop due to solution resistance was accessible introduces an error in the determination of this parameter. The nature of this error is further recognized by the observation that at higher concentrations there is a tendency of the peak potential to shift towards more positive values (in a positive scan) in comparison to the signal obtained from lower concentrations.

A more precise way of assessing the quality of the electrochemical response is to use the methods as proposed in [31] for SWV. The simplest of them consists in measuring the peak width at half height $W_{1/2}$, which should yield for the instrumental parameters and conditions used in this study 96 mV. Table 2 summarizes the typical results for this parameter for the transference of TMA$^+$; a slight broadening of the signal is observed throughout as expected for the reasons outlined in the previous paragraph.

An important feature of measuring the peak widths at half height is the resemblance that these determinations have when compared to traditional chromatographic methods, where the resolution of two close signals can be obtained through this parameter. Deviations from the ideal behavior have been observed in other ion transfer experiments in which IR compensation plays an important role [32]. However, as it will be discussed in the following section, the participation of other factors such as the difference in the diffusion coefficients of the ion in aqueous and nitrobenzene media shows to be of relevance.
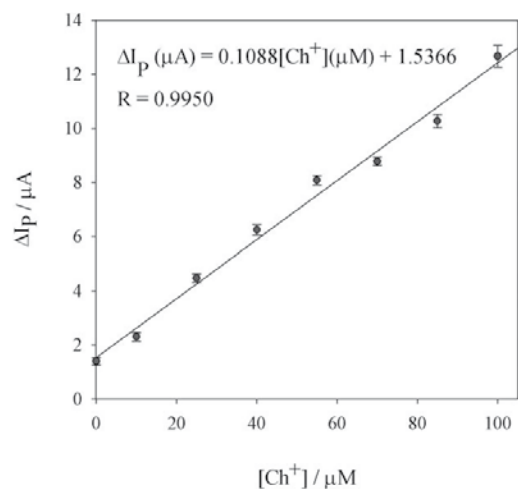
Concentration dependence of the SWV signal

The linear response of the SW Voltammetric peak current against concentration of the analyte in the aqueous phase is shown in Figures 3, 4 and 5 according to the expected behavior predicted by Equation 1. Good agreement with the linear model is further deduced from the high correlation coefficients (R) as seen in the inlets of the figures mentioned. Non-zero intercept values obtained are ascribed to the presence of a non-faradaic capacitive current which arises from the sweeping potential during a SWV experiment [33]. The capacitance values consistent with the intercept currents are in the order of 10 μF. Although the correspondence to a linear behavior is evident, there are two observations that are noteworthy.
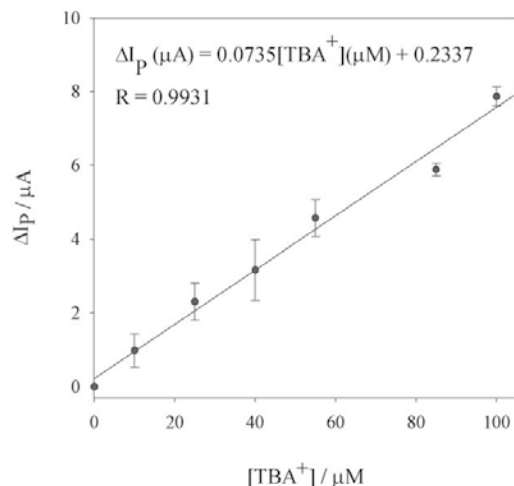
Figure 5. Peak differential current versus ion concentration for the transference of TBA$^+$. The background was subtracted in order to obtain a clear signal, thus the origin of the graph is fixed at zero in accordance to the ULA2 method. Data for the value of TBA$^+$ = 70μM not available. Each point corresponds to a total of 6 runs in 2 different experiments, error bars indicate ± standard deviation.

First, in general terms, the slopes obtained from the graphs are lower than the theoretical ones actually predicted by Equation 1. For instance, in the case of the transfer of TMA$^+$ the expected slope is 0.1674 μA/μM taking the value of 10.7 × 10^{-6} cm^{2}s^{-1} for D_i in aqueous phase [34], while the obtained value by experiment accounts for roughly two thirds. Equation 1 deals with the case in which the diffusion coefficient of the transferred species in both solvents is the same, however this case is not true in the system under study. A simple relation based on the Stokes-Einstein approximation [35] in terms of the diffusion coefficient follows:

$$\frac{\eta_1}{\eta_2} = \frac{D_{i,1}}{D_{i,2}} \qquad (2)$$

where η_j is the viscosity of the solvent j = 1 or 2, and $D_{i,j}$ is the diffusion coefficient of the species i in the solvent j.

The relation suggests that the diffusion coefficient values may differ significantly. Although this approximation could result an overestimation while not considering ion solvation effects, it provides an explanation to the differences between the theoretical and observed quantities.

For example, at 20 °C the viscosity for nitrobenzene is 2.03 × 10^{-3} kg m^{-1}s^{-1} and 1.002 × 10^{-3} kg m^{-1}s^{-1} for water (1 cP = 10^{-3} kg m^{-1}s^{-1}) [36]. Therefore, according to equation 2, the diffusion coefficient of an ion such as TMA$^+$, which is reported to transfer nonhydrated [37], is predicted to be twice as large in the aqueous phase than in the organic phase. It is important to keep in mind that the differential current (ΔI) in SWV is a product of a forward voltage ramp with an applied reverse pulse. In the scan direction selected for this study, the forward ramp will transfer the species from the aqueous into the organic phase while the reverse pulse will reestablish previous

conditions. Clearly an asymmetry in the values of the associated currents arises because of the different diffusional rates at which charge is transferred in both directions. By noticing that SWV in this case is especially sensible to these differences, it may also be interesting to point these results in the context of the reports of slowdown effects of the transfer of ions across an ITIES [38]. While this apparent loss in sensitivity in the technique may seem a drawback on its analytical performance, it is of special interest to note that the peak signal under the instrumental conditions used is equivalent to the one that would be obtained by cyclic voltammetry at a scan rate of 80 mV/s according to the Randles-Sevcik equation. The mentioned scan rate in CV may not result suitable for analytical purposes because of a large increase in the capacitive current with respect to the signal of ion transfer.

The second observation deals with the concentration range that is accessible to the technique. The authors considered proper to only introduce concentrations equal or below the 100 μM since higher concentrations often lead to a distortion of the SWV signal (as evaluated from $W_{1/2}$) and an apparent loss in sensitivity for the electrochemical signal, as well as a very high variation in ΔI_p between different runs. It is of our knowledge that similar studies have fit the experimental data of Differential Pulse Voltammetry analysis to a logarithmic function [29, 39, 40] however we discard this option when certainly these discrepancies from the expected behavior may arise from errors due to the uncompensated resistance or a saturated signal.

When high currents due to a high concentration of the analyte are registered, the potential drop due to the uncompensated resistance will tend to accentuate. This renders the subtraction procedure in SWV untrue as the association of a current to a given potential, which is of key importance for the algebraic treatment of the data, becomes uncertain. While exploring higher concentration limits may seem important, it would also carry within the need to increase the supporting electrolyte concentrations as to minimize migrational current effects, which in turn would lead to an undesirable increase in the background currents.

From another point of view, the fact that with the technique used in this study, low concentrations of analyte provide distinguishable bell-shaped responses is far more advantageous. Concentrated samples can be diluted thus decreasing matrix effects. Another alternative is to use a technique such as CV at higher concentrations and turn to SWV when the low concentration limit is reached. In order to verify the validity of our arguments on these two observations, SWV simulations were carried out using the DigiElch 2.0 software. The process was modeled as an electrochemical reaction in which the oxidized and reduced species have different diffusion coefficients in analogy to an electron transfer reaction.

The values for the diffusion coefficients of TMA$^+$ in nitrobenzene and water respectively were taken as $D_{i,NB}$ = 5.5 × 10^{-6} cm^2/s and $D_{i,W}$ = 10.7 × 10^{-6} cm^2/s from interpolation of the data in [34]. The uncompensated resistance was assumed 800 Ω in accordance with a typical value for our experiments and the capacitance of the interface was set at 14.5 μF by adjusting
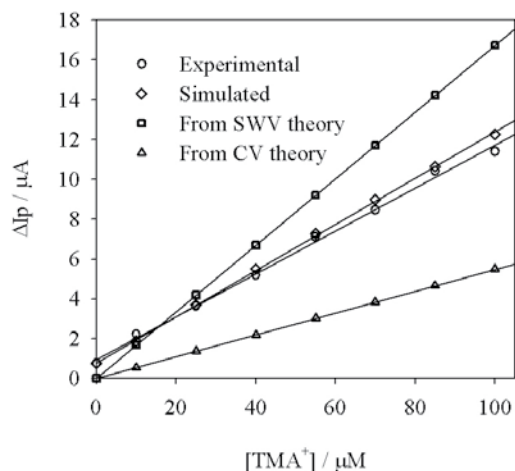
Figure 6. Comparison between simulated ($\Diamond$), experimental ($\circ$), SWV theory ($\square$) and CV theory (Δ) for the peak differential or peak currents. Scan rate for CV is 20 mV/s, comparable to the product of the frequency times the scan increment used in this study (10 Hz and 2 mV respectively). SWV and CV theory curves were obtained from Equation 1 and the Randles-Sevcik equation respectively and do not take into account background currents.

the background current for the simulation to a typical value obtained experimentally. The rest of the instrumental and cell parameters were taken as reported in the experimental section. Figure 6 shows the results of the simulations for the differential peak current and compares them to the experimental results and the results expected from SWV and CV theory taking only the diffusion coefficient in the aqueous phase. An interesting result from the simulations shown in Figure 6 is the loss in sensitivity that arises from the different diffusion coefficients of the species, as expected from the discussion in previous paragraphs. While indeed this loss in sensitivity causes the electrochemical signal to be smaller than the predicted by SWV theory, it is still higher than that of CV under similar conditions.

The statistical analysis for the data presented in Figures 3, 4 and 5 was made according to the Upper Limit Approach type-2 method (ULA 2) [41]. While this method gives usually higher values for the Limits of Detection and Quantification (LOD and LOQ respectively) than other more conventional approaches, the authors believe that subjecting the experimental data to such a strict model should account well for the varying nature of the measurements. While there are many sources of error as discussed previously, it is of the best intention to provide the most reliable analysis. According to this method the LOD and LOQ are calculated through Equations 3 and 4 as follows:

$$LOD = \left(\frac{t(\nu,\alpha)s_y}{q_1}\right)\left(1 + \frac{1}{n} + \frac{\bar{c}^2}{\sum_{i=0}^{n}(c_i - \bar{c})^2}\right)^{1/2} \quad (3)$$

$$LOQ = 3\left(\frac{t(\nu,\alpha)s_y}{q_1}\right)\left(1 + \frac{1}{n} + \frac{\bar{c}^2}{\sum_{i=0}^{n}(c_i - \bar{c})^2}\right)^{1/2} \quad (4)$$

Table 3. Standard error of estimates (s_y), limit of detection (LOD) and limit of quantification (LOQ) for the linearization in Figures 3, 4 and 5.

Species	s_y	LOD/μM	LOQ/μM
TMA+	0.2_3	5.9	17.9
Ch+	0.4_2	10.7	32.2
TBA+	0.3_5	13.8	41.5

where $t(\nu,\alpha)$ represents the value of Student's t for ν degrees of freedom and in this case it was used a significance level with $\alpha = 0.05$, n is the number of points in the graph, $\bar{c}$ is the mean of the concentrations used and c_i is a given concentration. The standard error of estimate, s_y, was obtained through a regression analysis. The results of the statistical analysis are summarized in Table 3. It is noteworthy that in the case of TMA$^+$, being an ion whose signal can be considered not to overlap the potential window, the LOD and LOQ are much more convenient, as expected from the consideration that its electrochemical signal is not subject to the variations in the background electrolyte transfer signal. As a comparison with other less strict methods of data analysis, we could follow the calculation of LOD and LOQ as 3 and 9 times respectively the standard deviation of the background. In the case of the average potential at which TMA$^+$ transfers, these figures account for an LOD of 1.5 μM and a LOQ of 4.6 μM. These results are comparable to others reported [28, 29, 42].

Temperature dependence of the SWV signal

Experiments were performed at several temperatures. First in blank conditions, Figure 7 shows the profile of the background current at different temperatures. The most important observation in this figure for analytical applications is the practically null increase in background current in a wide flat region comprised in the 0.25-0.6 V interval. The limits of this region account for the transference of the supporting electrolytes.
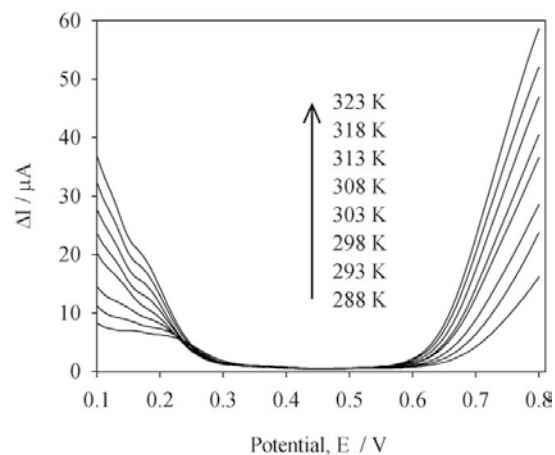

Figure 7. Evolution of the SWV signal for the background current at increasing temperatures. The flat region of the potential window remains practically unchanged by the variation of temperature.

A trend is clearly observed by noticing that at higher temperatures the signal from the supporting ions increases; this trend is expected as at higher temperatures there is an increase in the diffusion coefficient of the species involved, we will elaborate this point further in the discussion for the species of interest for this study. At this point however, the main feature in Figure 7 is that a change in temperature will not alter significantly the background current for the mentioned interval, whereas a change in instrumental parameters such as f and E_{SW} in SWV or the scan rate in CV would. Figure 8 shows a profile of SW voltammograms for the transference of TMA^+ with a fixed concentration and different temperatures. The gridlines in the graph allows visual inspection, and it can be observed that there is an increase in ΔI_p at increasing temperatures. Less evident is a displacement of the peak potential towards less positive values at increasing temperature. As expected from the analysis of Figure 7, the background signal corresponding to the flat region of the voltammograms remains practically unchanged upon the variation in temperature.

Figure 9 shows the peak potential displacements obtained for the series of SW voltammograms for the transference of TMA^+. The trend in this graph is evident, although deviations are noticeable by the extent of the error bars and the lack of fitting of the last point. These errors are mostly attributed to differences in the thermal behavior of all the components of the system (i.e. the interface, the reference electrodes, the solutions, etc.) from run to run. In the case of Ch^+ and TBA^+ the trend is also observed. The net displacement accounts for about 50 mV in the whole range studied. The change in peak current with respect to temperature is analyzed in Figure 10; the experiments show that data follow a linear trend, being the slope of the graph equivalent in magnitude to the one obtained by variation of the concentration as shown in Figure 3; thus roughly a change
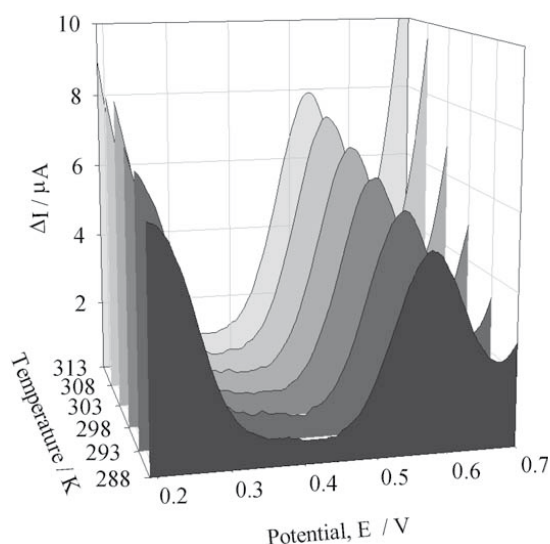

Figure 9. Variation of the cell peak potential for the transfer of TMA^+ $50\mu M$ at different temperatures. The point at 313K is shown but not taken into consideration for the regression.
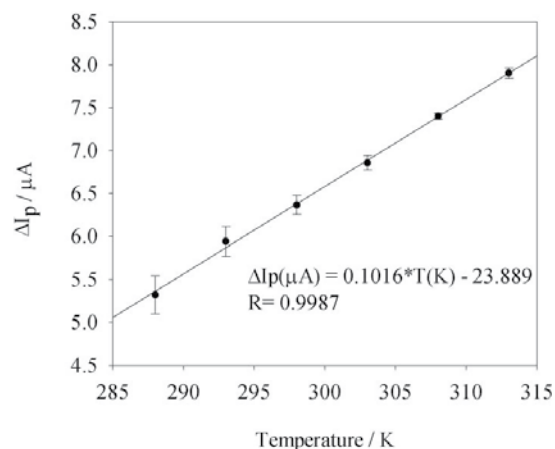
Figure 10. Differential peak current for the transfer of TMA^+ $50\mu M$ at different temperatures. A linear fit is obtained for the range studied. The intercept in this figure has no physical meaning.

in one unit of temperature (in Kelvin) is equal to a change in one micromolar unit of concentration. An obvious advantage of this is that while the background currents do not increase significantly, the peak current does so at easily accessible temperatures in the experiment, therefore increasing notoriously the sensitivity of the method. As explained in the experimental section, the interface was controlled so that it always remained flat from one temperature to another, so that the area does not change from one measurement to the other.

The increase in ΔI_p then truly represents to be substantial for the relation of signal to background.

While other conventional techniques such as CV will exhibit a similar increase in the measured current at higher temperatures, let the comparison be made to evaluate the combined effect of using SWV at high temperatures: in order to achieve the peak current observed for Ch^+ at the highest temperature

Figure 8. Evolution of the SWV signal for the transfer of TMA^+ $50\mu M$ at increasing temperatures. The change in peak parameters is evident; while the peak potential displaces towards less positive values there is an increase of the peak differential current that nearly doubles in value going from 288K to 313K.
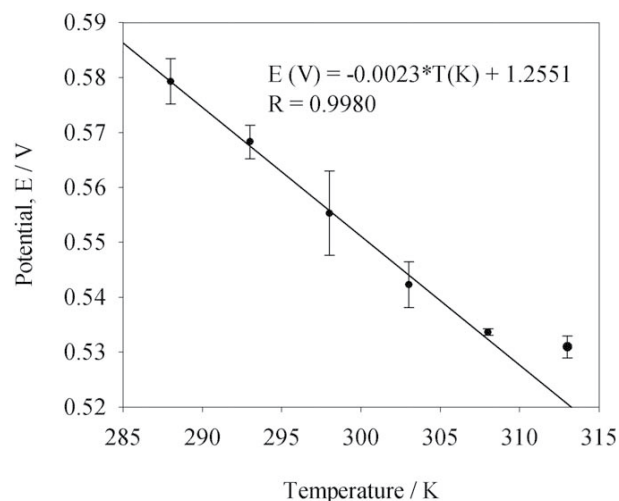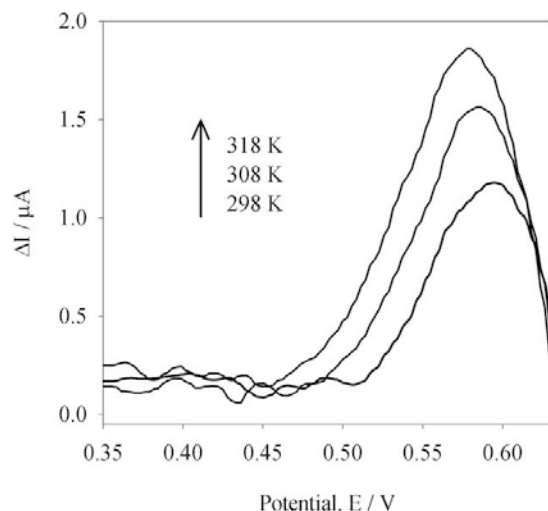
Figure 11. Enhancement of the SWV signal for the transfer of Ch^+ at increasing temperatures. The background signal is subtracted for clarity. There is a 75% increase in the original signal when raising the temperature.

in Figure 11, roughly a scan rate of 220 mV/s would be necessary at 25 C to attain the same signal with CV, which of course would turn the analysis most difficult because of the large increase in the capacitive current.

Conclusions

In conclusion, the analysis by Square Wave Voltammetry of the Tetramethylammonium (TMA^+), Choline (Ch^+) and Tetrabutylammonium (TBA^+) cations as representatives of quaternary ammonium ions was succesfully performed and showed some interesting features that render it useful for analytical determinations. Well defined and characterizable waves were obtained for the transfer of these ions; when a substantial degree of overlap was observed, as in the case of TBA^+ a background substraction allowed the observation of the corresponding ion transfer signal. While it is true that overlapping with the background signal introduces a significant amount of error in the accurate determination of the electrochemical signal, good results are obtained for the TMA^+ and Ch^+ ions, whose peak parameters fall well into the planar region of the potential window (slightly overlapping in the case of Ch^+). Good resolution is obtained for the analysis of the transfer signal of two ions of interest even within the same run provided their afinity towards a given phase is different enough, as in the case of TBA^+ and Ch^+. The differential peak current obtained by SWV at the moderate instrumental parameters used in this study shows an enhancement with respect to more conventional techniques such as CV even though the electrochemical signal is lower than the expected values according to SWV theory. The differences in the behavior of the ions in the two phases (specially the diffusion coefficient) may well account for the discrepancies with theory. More insight into the details of the ion transfer must
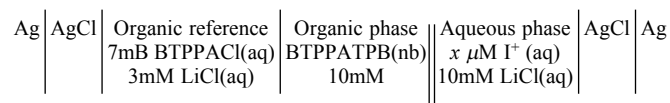
be addressed in order to solve the differences, however from a pragmatic point of view, better results for the implementation of the technique of simple ion transfer for sample analysis can already be accesed through the use of SWV.

A further increase in sensitivity was shown by raising the temperature of the system: while the electrochemical signal arising from the ion transfer of the analyte increased substantially, little variation is observed from the background signal in the planar region of the potential window. This sets a new dimension that can be exploited to attain lower detection and quantification limits. The thermal behavior of the peak parameters shows a linear dependence with respect to temperature, which is useful when the analysis requires a reference to a given temperature. We also regard these results important in the sense that they may help us understand into a greater depth the physico-chemical nature of the ion transfer.

Experimental

Chemicals and electrochemical cell

All aqueous solutions were prepared using deionized water obtained from an EasyPure II water deionizer and saturated with nitrobenzene prior to use. Nitrobenzene 99% (Aldrich) was used as received; the solutions prepared with this solvent were isolated from light in order to avoid changes in color as observed after one week of exposition. Tetramethylammonium chloride (TMACl), tetrabutylammonium chloride (TBACl), sodium tetraphenylborate (NaTPB), bis-(tripheny-lphosphor anylidene)ammonium chloride (BTPPACl), silver wire from Aldrich(USA), LiCl, HCl, KCl, $NaHCO_3$ from Baker(USA) and choline chloride (ChCl) from The Biochemical Corporation (USA) were used as received. Bis-(triphenylphospho-ranylidene) ammonium tetraphenylborate (BTPPATPB) was synthesized as reported in reference [25, 43]. The interface chosen for this study was the water/nitrobenzene using BTP-PATPB and LiCl as supporting electrolytes for the organic and aqueous phase, respectively. The chlorides of three model quaternary ammonium ions were used for the study based on their affinity to either phase in the elected system: choline (Ch^+) as a very hydrophilic ion, tetramethylammonium (TMA^+) as a moderately hydrophilic ion and tetrabutylammonium (TBA^+) as a rather hydrophobic ion. The cell used throughout the experiments can be described as follows:

Ag	AgCl	Organic reference 7mB BTPPACl(aq) 3mM LiCl(aq)	Organic phase BTPPATPB(nb) 10mM	Aqueous phase x μM I^+ (aq) 10mM LiCl(aq)	AgCl	Ag

The interface of interest is noted by using a double bar, the subscripts (nb) and (aq) refer to organic and aqueous solutions while the use of I^+ in the aqueous phase refers to the ion of interest. The electrochemical cell was made out of glass and allowed the accommodation of two Luggin capillaries in which the flat interface was positioned to the best extent possible

halfway the distance between them. The geometrical area of the interface was 45 mm^2 and the volume of both phases was set to a constant value of 1.5 mL in all experiments. Two working electrodes consisted of two Pt wires sealed in glass capillaries such as to expose 1 cm of the wire to be in contact with each of the respective phases. Ag/AgCl electrodes were prepared prior to each experimental session by electrolysis of a silver wire in a 0.1 M KCl solution. The use of LiCl and BTPPATPB renders a potential window in which the transfer of the selected ions can be studied either by direct inspection or by subtraction of the background response. The high concentration of supporting electrolyte relative to that of the ion of interest (typically in the range 10μM to 100μM) was chosen on the basis of minimizing the migrational response of the ions of interest and at the same time ensuring a proper conductivity in each phase, however not as high as to making the ion transfer signal to background ratio unpractical. In the case of the organic/organic reference junction, similar concentrations of the BTPPA$^+$ ion in both sides allow a correct functioning of the organic reference. The concentration of BTPPACl is also near the saturation point in water at 298 K.

Instrumentation and instrumental parameters

All electrochemical measurements were carried out using an EG&G PARC potentiostat model 273A provided with an external differential electrometer which allows a 4-electrode configuration. The glass cell was immersed in a water bath in contact with a glass jacket whose temperature control was provided by a MGW-Lauda R18 external circulator. The glass jacket was optically and thermally isolated using a polystyrene cover. Both the electrometer cage and the mounted cell were kept inside a grounded Faraday cage. The temperature was monitored with a precision of ±0.5 °C at close proximity to the electrochemical cell. Experiments to determine concentration versus SWV signal relation were conducted at 298 K while temperature dependent experiments were performed in the range of 288 to 313 K; temperature stabilization was allowed until no fluctuations were observed.

The instrumental parameters for the SWV technique chosen for this study were a scan increment of 2mV, frequency (f) of 10 Hz and a square wave pulse amplitude (E$_{SW}$) of 20 mV to ensure that the voltammetric signal was as symmetrical as possible with the smallest interference of the background, as interpreted by a maximum width of the potential window; the chosen parameters are similar to the ones used in other SWV study at the ITIES [28]. All potential measurements are reported to the cell potential as given by the reference electrodes. The scanned potential range was between 0.1 V and 0.8 V in accordance to the extent allowed by the electrochemical window; typical open circuit potentials ranged from 0.15 V to 0.17 V. IR Compensation was performed in each experimental run in the positive feedback mode with 80% of compensation level; attempts to increase the compensation level often led to severe ringing and thus were avoided. Typical uncompensated resistances were in the range 600 to 1000 Ω and were seen to depend greatly on the position of the interface respective to

the Luggin capillaries; however the narrowing of this range of compensations was often compromised by the loss of flatness of the interface. For the temperature dependent experiments a curving of the interface was observed at increasing temperatures; this was corrected however by modifying slightly the hydrostatic equilibrium of the electrochemical cell until flatness of the interface was recovered.

Acknowledgements

References

1. Iglesias, R.; Dassie, S. *Adv. Chem. Res.* **2010**, *3*, 121-192.
2. Dryfe, R.A.W. *Adv. Phys. Chem.* **2009**, *141*, 153-215.
3. Vanysek, P.; Ramirez, L. *J. Chil. Chem. Soc.* **2008**, *53*, 1455-1463.
4. Samec, Z.; Samcová, E.; Girault, H.H. *Talanta* **2004**, *63*, 21-32.
5. Reymond, F.; Fermin, D.; Lee, H.J.; Girault, H.H. *Electrochim. Acta* **2000**, *45*, 2647-2662.
6. Senda, M.; Kakiuchi, T.; Osakai, T. *Electrochim. Acta* **1991**, *36*, 253-262.
7. Arugonda, S.K., International programme on chemical safety, poisons information monograph G022 (1999) http://www.inchem.org/documents/pims/chemical/pimg022.htm. Accessed on May, 2012.
8. Gurjinder, K.; Hrabetova, S.; Guilfoyle, D.N.; Nicholson, Ch.; Hrabe, J. *J. Neurosci. Meth.* **2008**, *171*, 218-225.
9. Vorísek, I.; Syková, E. *J. Neurophysiol.* **1997**, *78*, 912-919.
10. Covello, M.; Schettino, O. *Il Farmaco* **1967**, *21*, 145-159.
11. Giovannelli, D.; Aballe, F.; Labnova, S.r.L. *J. Chromatogr. A* **2005**, *1085*, 86-90.
12. Bourque, A.; Clark, S.P.; Kloss, A.; Wang, B.H.; Cohen, A.S. *Anal. Chem.* **2005**, *77*, 2810-2817.
13. Wang, L.H. *J. Chromatogr. Sci.* **2002**, *40*, 326-330.
14. Rasulev, U.K.; Nazarov, E.G.; Khudaeva, G.B. *J. Chromatogr. A* **1995**, *704,* 473-482.
15. Para, B.V.; Nunez, O.; Moyano, E.; Galceran, M.T. *Electrophoresis* **2006**, *27*, 2225-2232.
16. Ding, X.; Zhao, R.; Zhao, S.; Kang, J. *Sepu* **2003**, 21, 520-523.
17. Taylor, R.B.; Toasaksiri, S.; Reid, R.G. *J. Chromatogr. A* **1998**, 798, 335-343.
18. Matysik, F.; Marggraf, D.; Glaser, P.; Broekaert, J.A.C. *Electrophoresis* **2002**, *23*, 3711-3717.
19. Tang, F.P.W.; Leung, G.N.W.; Wan, T.S.M. *Electrophoresis* **2001**, 22, 2201-2209.
20. Heinig, K.; Vogt, C.; Werner, G.; *J. Chromatogr. A* **1997**, 781, 17-22.
21. Johnson, B.; Grinberg, N.; Bicker, G.; Ellison, D. *J. Liq. Chromatogr. R.T.* **1997**, *20*, 257-272.
22. Nunez, O.; Moyano, E.; Galceran, M.T. *J. Chromatogr. A* **2002**, *974*, 243-255.
23. Carneiro, M.C.; Puignou, L.; Galceran, M.T. *Anal. Chim. Acta* **2000**, *408*, 263-269.
24. Pivarnik, L.F.; Ellis, P.C.; Wang, X.; Reilly, T. *J. Food Sci.* **2001**, *66*, 945-952.
25. Samec, Z. *Pure Appl.Chem.* **2004**, *76*, 2147-2180.

26. Marecek, V.; Samec, Z.; Koryta, J. *Adv. Colloid Interface Sci.* **1988**, *29*, 1-78.

27. Pereira, C.M.; Silva, F.; *Electroanalysis* **1994**, *6*, 1034-1039.

28. Sherburn, A.; Arrigan, D.; Dryfe, R.; Boag, N. *Electroanalysis* **2004**, 16, 1227-1231.

29. Beni, V.; Ghita, M.; Arrigan, D. *Biosens. Bioelectron.* **2005**, 20, 2097-2103.

30. Molina, A.; Ortuno, J.A.; Serna, C.; Torralba, E.; Gonzalez, J. *Electroanalysis* **2010**, 22, 1634-1642.

31. Aoki, K.; Maeda, K.; Osteryoung, J. *J. Electroan. Chem.* **1989**, *272*, 17-28.

32. Kakiuchi, T.; Noguchi, J.; Kotani, M.; Senda, M. *J. Electroan. Chem.* **1990**, *296*, 517-535.

33. Shan, X.; Shaopeng, W.; Wang, W.; Tao, N. *Anal. Chem.* **2011**, *83*, 7394-7399.

34. Wandlowski, T.; Marecek, V.; Samec, Z.; Fuoco, R. *J. Electroanal. Chem.* **1992**, *331*, 765-782.

35. Fürth, R. (Ed), Einstein, A. *Investigations on the Theory of Brownian Movement*, Dover Publications Inc, New York, NY, USA, **1956**.

36. Weast, R.C. (Ed), *Handbook of Chemistry and Physics 67th ed.,* CRC Press, Boca Raton, FL, USA, **1986**.

37. Osakai, T.; Ogawa, h.; Ozeki, T.; Girault, H.H. *J. Phys. Chem. B* **2003**, *107*, 9829-9836.

38. Kornyshev, A.A.; Kuznetsov, A.M.; Urbakh, M. *Russ. J. Electrochem.* **2003**, *39*, 119-125.

39. Zhan, D.; Mao, S.; Zhao, Q.; Chen, Z.; Hu, H.; Jing, P.; Zhang, M.; Zhu, Z.; Shao, Y. *Anal. Chem.* **2004**, *76*, 4128-4136.

40. Qian, Q.; Wilson, G.S.; Bowman-James, K.; Girault, H.H. *Anal. Chem.* **2001**, *73*, 497-503.

41. Mocak, J.; Bond, A.M.; Mitchell, S.; G. Scollary. *Pure Appl. Chem.* **1997**, *69*, 297-328.

42. Lee, H.J.; Beriet, C.; Girault, H.H. *Anal. Sci.* **1998**, *14*, 71-77.

43. Gobry, V. *Ion Transfer of Acids and Bases*, Thesis EPFL (**2001**).